Full Paper Transactions, SMiRT 28
Toronto, Canada, August 10-15, 2025

FULL-SIZE THERMAL FATIGUE PIPE TEST WITH NON-DESTRUCTIVE AND DESTRUCTIVE DAMAGE CHARACTERIZATION

Klaus Heckmann[1], Nina Grözinger[2], Georg Veile[3], Kai Donnerbauer[4], Luca Alexander Koch[5], Jens Arndt[6], Jürgen Sievers[7], Stefan Weihe[8], Frank Walther[9], Peter Starke[10], Viktor Lyamkin[11], Fabian Weber[12], Christian Boller[13]

[1] Group Head, GRS, Köln, Germany (klaus.heckmann@grs.de)
[2] Research Assistant, Materials Testing Institute (MPA) University of Stuttgart, Stuttgart, Germany
[3] Research Assistant, Materials Testing Institute (MPA) University of Stuttgart, Stuttgart, Germany
[4] Research Assistant, TU Dortmund University, Dortmund, Germany
[5] Research Assistant, TU Dortmund University, Dortmund, Germany
[6] Technical Expert, GRS, Köln, Germany
[7] Senior Expert, GRS, Köln, Germany
[8] Director, Materials Testing Institute (MPA), University of Stuttgart, Stuttgart, Germany
[9] Professor, TU Dortmund University, Dortmund, Germany
[10] Professor, University of Applied Science Kaiserslautern, Kaiserslautern, Germany
[11] Postdoctoral Researcher, University of Applied Science Kaiserslautern, Kaiserslautern, Germany
[12] Group Head, University of Applied Science Kaiserslautern, Kaiserslautern, Germany
[13] Professor, Saarland University, Saarbrücken, Germany

ABSTRACT

While thermal fatigue is a safety-relevant phenomenon in nuclear engineering and a key motivation for experimental and simulative fatigue research, fatigue resistance of materials is usually characterized by mechanical tests in laboratory. In this paper, the fatigue loads are applied by actual thermal fluctuations in a piping test rig. The austenitic stainless steel AISI 347 pipe under these thermal fatigue loads is characterized by simulations as well as non-destructive and destructive experimental techniques.

INTRODUCTION

Thermal fatigue, i.e. the cyclic loading of structure due to temperature fluctuations, is a relevant degradation mechanism in the piping system of nuclear power plants (Ballesteros et al., 2014, NEA, 2019). Typical causes for thermal fatigue loading are operational cycles, mixing phenomena at T-junctions, injection nozzles, or thermal stratification phenomena in dead-end pipe branches (Lydell et al., 2021). This motivates the need for a fatigue life prediction and fatigue monitoring techniques.

The fatigue resistance of piping materials is usually characterized by mechanical tests in laboratory on material specimens, at specified temperature and medium conditions. This approach allows for a characterization of environment assisted fatigue, see e.g. Solin (2024) and Solin and Seppänen (2024). However, this setup only takes place under idealised laboratory conditions. Component-level full-size tests are more demanding to the experimental design and therefore rarely carried out (a recent investigation can be found in Hong et al., 2023).

In this paper, a full-size test of an austenitic stainless steel pipe under thermal fatigue loads, and the characterization of the damage by non-destructive and destructive techniques is presented. While with a mechanical specimen fatigue test the characterization of loads can be measured accurately, the use of a piping test rig implies that the derivation of the actual fatigue load in the test poses first challenges.

Therefore, in order to retrieve sufficient information about the fatigue degradation in the test, a complex evaluation program around the actual component test is imposed (see Figure 1).

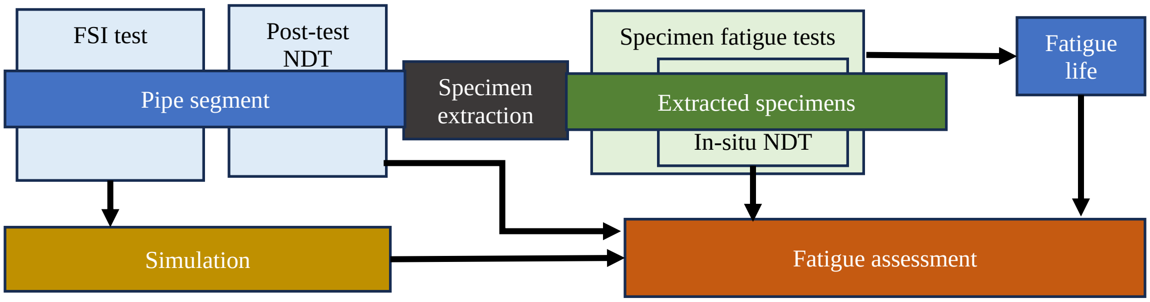

Figure 1. Scheme of component test, simulation, NDE, and specimen testing for the fatigue assessment.

This process is reflected by the structure of this paper. In the first section, the thermal fatigue test of the pipe segment is presented. After the test (and in addition, at test interruptions), non-destructive testing (NDT) is applied. The test conditions are monitored and used to calibrate simulations, which can link the test conditions to strain amplitudes. Next, the pipe component is sectioned by electrical discharge machining, and specimens are taken at defined locations. These specimens are then subjected to fatigue tests. The (reduced) fatigue life, together with in-situ NDT methods applied during the specimen fatigue tests, allows to finally assess the fatigue behaviour in the test. This allows for assessment of the locally reduced fatigue life.

THERMAL FATIGUE PIPE TESTS

The thermal fatigue tests are performed at the Fluid-Structure-Interaction (FSI) test rig at MPA Stuttgart University, a multi-purpose test facility which can be operated up to a pressure of 8.0 MPa at up to 280 °C temperature (Weihe et al., 2022, see Figure *2*). A 3-inch (DN 80) AISI 347 pipe section is inserted in the test rig.

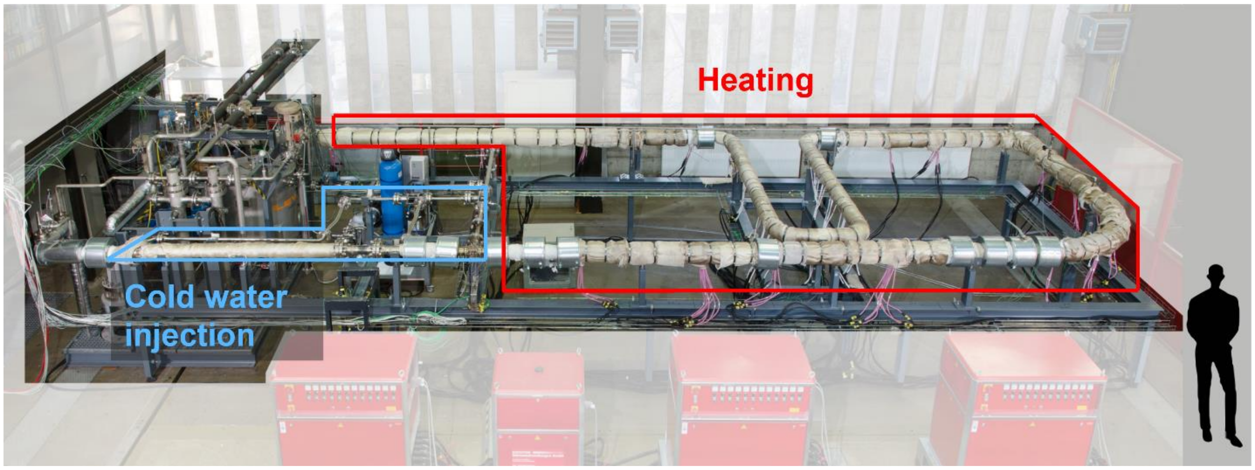

Figure 2. The fluid-structure interaction test rig with the cold water injection section

In this hot pressurized loop, cold water can be injected periodically by a cold water branch. This leads to the desired thermal cycles. To increase the thermal stresses in the pipe wall, an internal pipe nozzle is inserted in the test section directing the cold water injection directly to the internal pipe surface. Cold water injection nozzle and the internal pipe is shown in Figure 3.

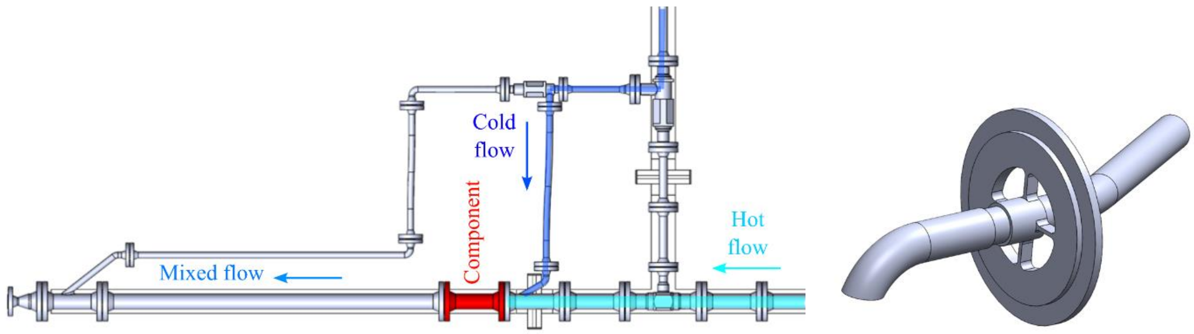

Figure 3. The fluid-structure interaction test rig with the cold water injection section (left), and a detail of the internal pipe (right).

This configuration leads to an asymmetric thermal loading of the inserted pipe, as only one side is in flow direction. Therefore, the different locations around the pipe circumference experience different thermal cycles. As the injected cold water forms naturally a cold layer at the pipe bottom due to the density difference, the injection is directed to the lower pipe surface. In the test, after completion of a certain number of cycles, the pipe section will be rotated by 180° to allow also the test of a second location with the same component. To visualize the convention with the angle and rotations, a drawing is provided in Figure 4.

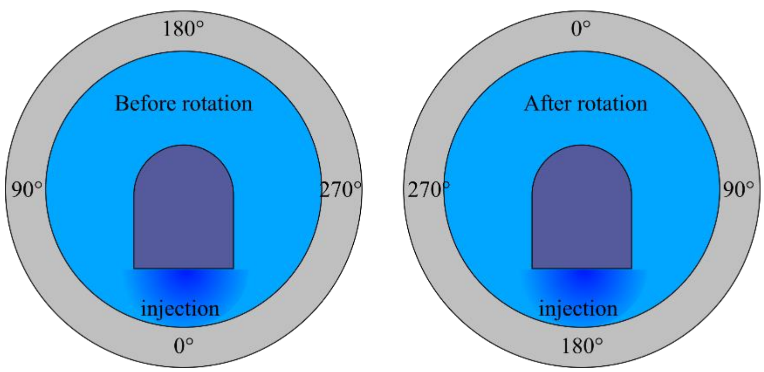

Figure 4. The orientation of the component test section relative to the cold water injection.

LOAD SPECTRUM ANALYSIS

The characterization of the associated strain amplitude is done by simulations (details found in Arndt et al., 2024). As the heat transfer in the test is a significant source of uncertainties, the simulation is calibrated to the temperature measurements in the test. Therefore, the measurement module equipped with thermocouples (see Figure 5), that are able to track the temperature change in the pipe wall, is essential.

The comparison of the measured temperature at one specified point in the wall with the calibrated simulation is shown in Figure 6 for three different cold water cycle durations of 15 s, 30 s, and 45 s.

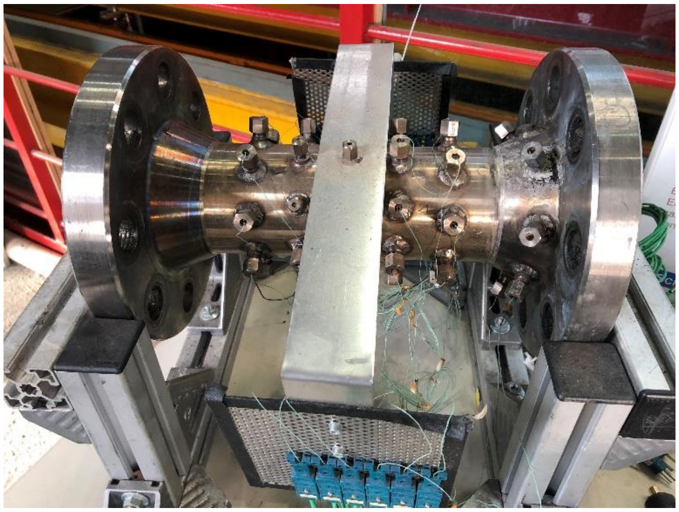

Figure 5. Measurement module with thermocouples, used for calibration of the simulation.

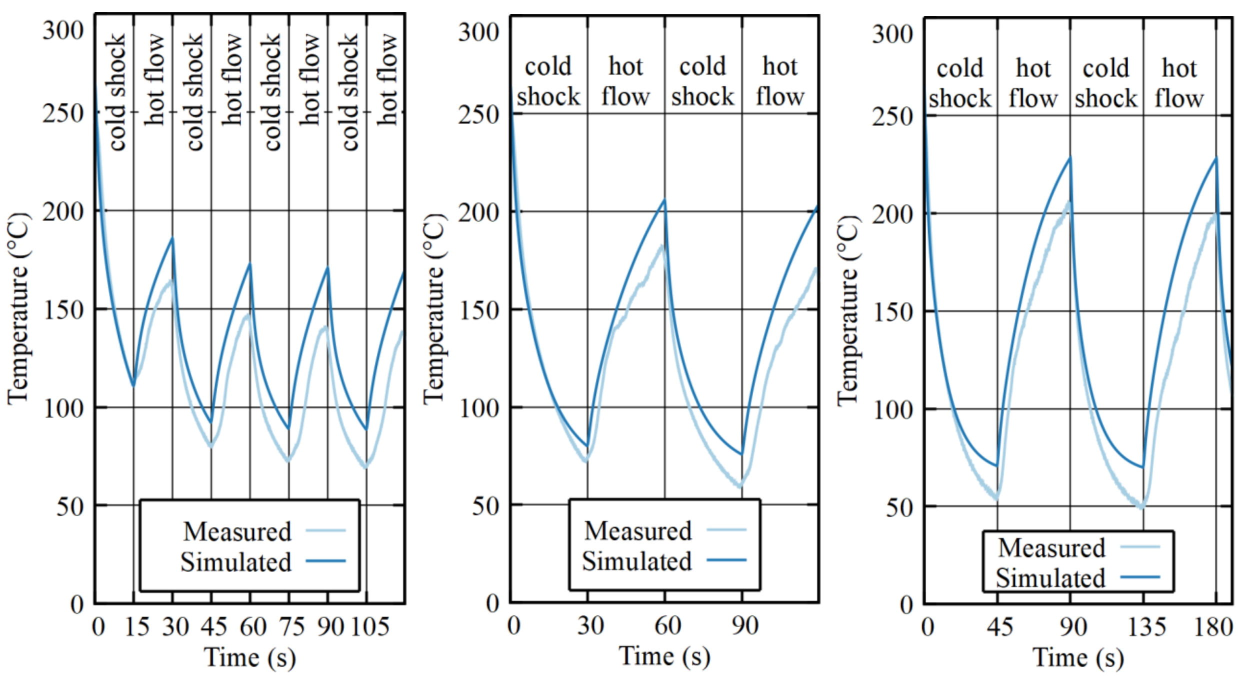

Figure 6. Comparison of measured and simulated/calibrated temperatures at one evaluation point.

This comparison shows that the duration of the cold shock has a significant impact on the temperature variation, from ~70-140 °C for 15 s over ~60-180 °C to ~50-200 °C for 45 s (at the evaluation point). This comparison shows also that the calibration approach with a single heat transfer coefficient is possible, but limited. A good example for the limits of the constant heat transfer coefficient approach is the deviation in the first reheating cycle in the 30 s interval: The first seconds show a good agreement between measurement and simulation, while the last seconds exhibit a clear deviation between both. This might be related to the complex flow conditions in the experimental setup.

This simulated temperature field is required to compute the time-dependent strains and stresses in the pipe section, with the consideration of the mechanical boundary condition, for deriving the fatigue-relevant strain amplitudes. The procedure for this and the complexity due to the relation to the destructive assessment is explained in detail by Arndt et al. (2024); the resulting strain amplitudes for two different cases are shown in Table 1.

Table 1: Strain amplitudes for different cycle durations.

Cycle interval		30 s	45 s
Strain amplitude	(%)	0.0935	0.103
Stress amplitude	(MPa)	167	184

This investigation shows that the optimization of the test cycle for obtaining a maximal fatigue degradation in a considered time is complex, since the fatigue life has a power law scaling with amplitude. However, the present experiment was performed with a 30 s cycle. Although the material is exposed to corrosive effects, the resulting strain amplitudes should not lead to crack initiation, since the threshold value of austenitic stainless steels and their welds are assumed to be 0.1% strain amplitude in corrosive high temperature water (Chopra and Stevens, 2018). Nevertheless, the material condition and microstructure can change at this load level due to cyclic stress and the metastability of austenitic stainless steels (Smaga et al., 2022).

POST-TEST NON-DESTRUCTIVE CHARACTERIZATION

Non-destructive evaluations based on eddy current testing (ECT) are performed after the test, and additionally at defined simulated component ages, when the testing is interrupted. This investigation allows for the test of capabilities of micromagnetic techniques (Heckmann et al., 2023, Donnerbauer et al., 2024) under realistic conditions. It has to be noted that the sensitivity of ECT techniques to fatigue influence in the metastable austenitic stainless steel AISI 347 is mostly related to deformation-induced martensitic transformation, which changes the electromagnetic properties of the microstructure that are easy to measure. This phase transformation occurs only at sufficiently low temperatures, and this raises the question if this transformation and its detectability are similar in thermal fatigue tests, where the temperature changes in time and volume all the time.

In contrast to Heckmann et al. (2023), the relevant information is not the temporal variation of the eddy current test, but the spatial variation. Moreover, since the fatigue degradation throughout the full pipe thickness is of interest, the excitation frequency has to be chosen such that the penetration depth δ is in the order of the wall thickness. This leads to frequencies in the range of 1.1 kHz (12.83 mm) to 2 kHz (9.51 mm), which is much lower than chosen for ECT during fatigue tests in the referred article. The spatial variation of the ECT for 1.1 kHz and 2 kHz at the start of the test, after 17.5k cycles, and after 35k cycles is shown in Figure 7. Thereafter, the test is continued with the rotated pipe component, and additional measurements are performed after additional 17.5k and 24.5k cycles.

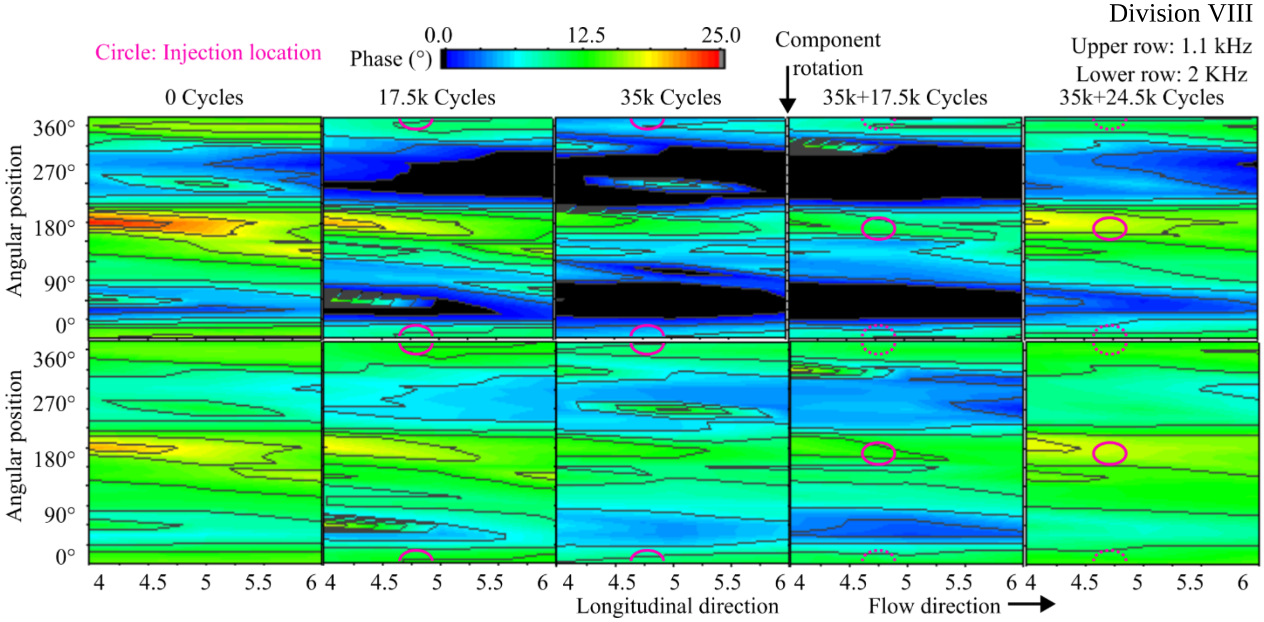

Figure 7. ECT map of the pipe surface, phase at 1.1 kHz (upper row) and 2 kHz (lower row), before, during, and after the test.

While the spatial variation of the ECT signal clearly exhibits specific longitudinal stipes, these should not be related directly to the influence of the cold water injection and the subsequently induced fatigue loads. First, the longitudinal inhomogeneities are already found before the thermal fatigue tests, and they are also found at locations which are not directly influenced by the injection (the 180°-stripe in the first three measurements). It is rather questionable if the observed variations between the different component states in the test interruptions are really caused by the thermal cycles – this observation would be in accordance with the conjunction that the temperatures are too high for the deformation-induced phase transformation, or that the component is still in a very early stage of the fatigue life, where almost no structural modifications can be detected.

FATIGUE TESTS ON EXTRACTED SPECIMENS

Specimen Extraction and Testing Setup

After the test, fatigue specimens are extracted from the pipe segment (see also Donnerbauer et al., 2024). The specimens are tested at constant amplitude until failure, to quantify the remaining fatigue life; the inclusion of specimens in the cold injection zone and out of the zone allows also for a comparison between these states. The comparison with unaged material allows to quantify the reduction in lifetime, which corresponds to the fatigue usage during the test. The extraction scheme and a photograph of the fatigue test setup is shown in Figure 8.

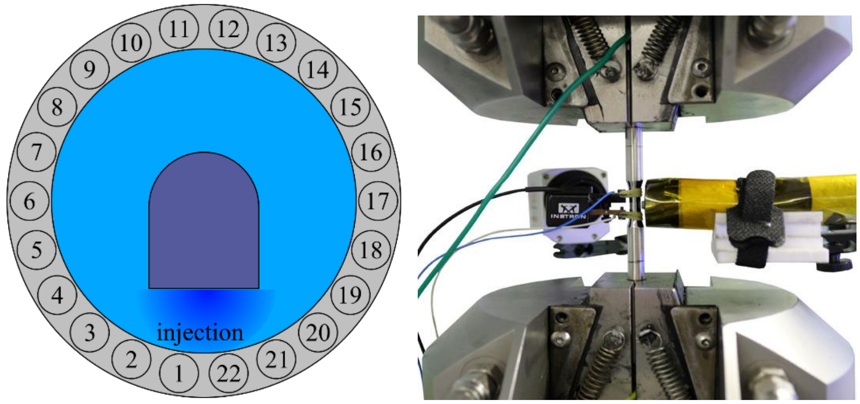

Figure 8. Extraction scheme of the specimens from the pipe segment
(left; injection location before rotation), and instrumented fatigue test setup (right).

The specimens designated as 1 and 22 are directly below the injection in the first part of the component test, while specimens labled 11 and 12 are in this region in the second part. The specimens around 6 and 17 were most distancedfurthest from the point of injection all the time.

In-situ NDE during Fatigue Tests

The investigation of sensor data during fatigue test is an interesting approach to understand microstructural fatigue behavior and monitoring options. In this case, the aim is to identify traces of the component test in the data. It is expected to identify differences especially in the beginning of the test, and as the thermometry and the resistometry are more sensitive for very high fatigue usage, the investigation is concentrated on the mechanical behavior and eddy current. These results are shown in the first ten cycles in Figure 9.

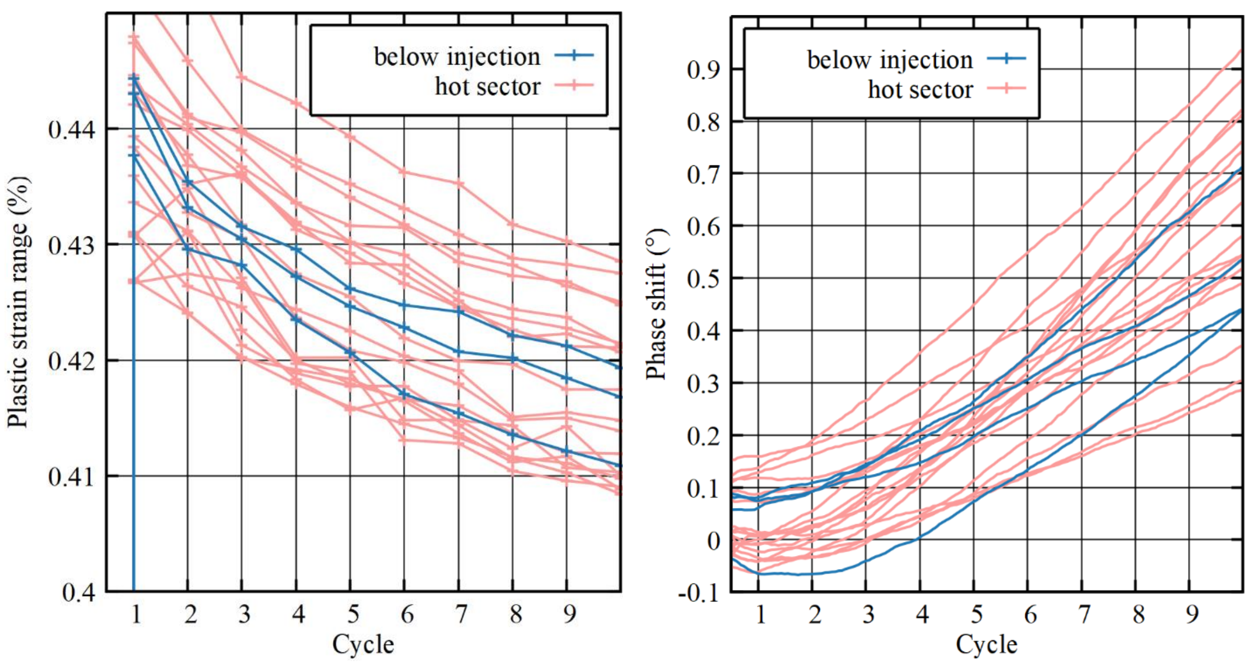

Figure 9. NDE signals during the first cycles of the extracted specimens.
Left: Plastic strain range, right: eddy current phase shift (500 kHz).

This comparison shows that the specimens extracted from the zone below the injection have practically no different NDE properties than the specimens from the other locations.

Fatigue Life of Extracted Specimens: Destructive Characterization

The extracted specimens are subjected to constant amplitude fatigue tests (room temperature, strain controlled, at 0.4 % total strain amplitude, 0.25 Hz) until failure. The number of cycles to failure for each angular location is shown in Figure 10; the injection locations are highlighted.

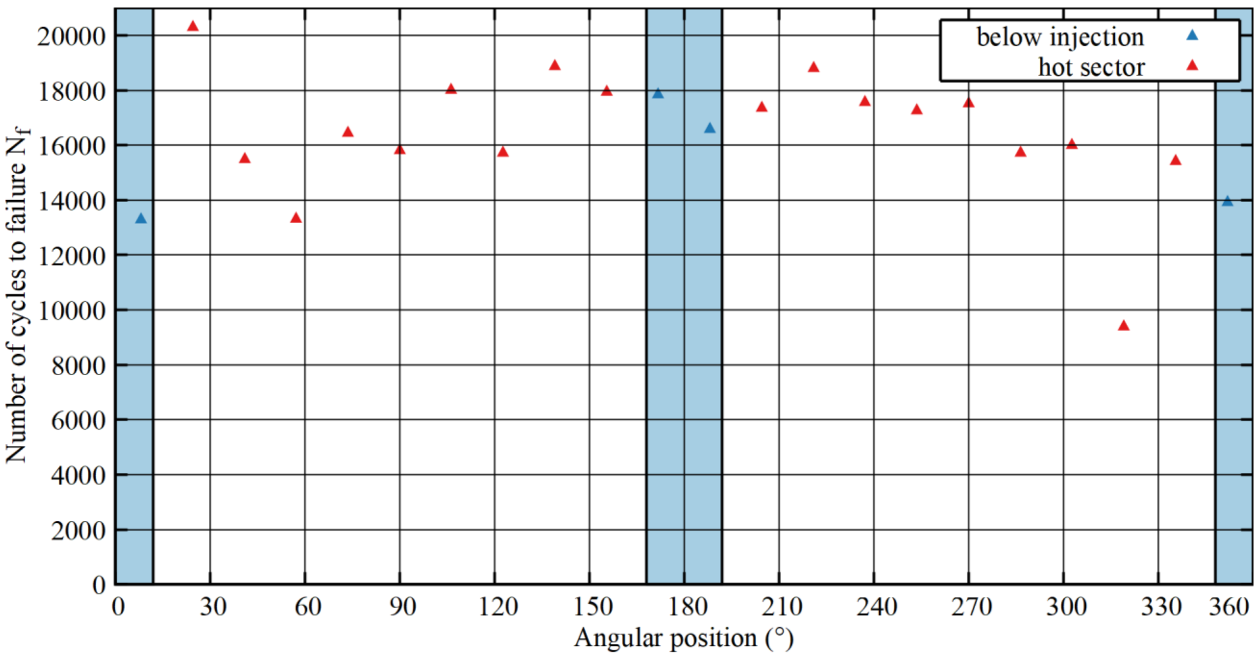

Figure 10. Number of cycles to failure for the extracted specimens (locations below injection shaded).

This comparison shows that there is a small trend to smaller number of cycles in the cold water injection sector, meaning the specimens in the hot sector vicinity have higher number of cycles to failure. However, two specimens in the hot sector (4 and 20) also show comparable reduced fatigue life, which can be reasoned with chemical inhomogeneities and their influence on fatigue life in austenitic stainless steels (Veile et al., 2024a).

FATIGUE ASSESSMENT

With help of the number of cycles to failure of the extracted specimens (at the defined strain amplitude in the test) and the computed strain amplitude in the preceding component test (in correspondence with the injection-induced thermal cycles in the test rig), the fatigue life can be studied in a fatigue diagram. As a reference for the austenitic stainless steel, data from Rudolph et al. (2024), Smaga et al. (2024), and Veile et al. (2024a, 2024b) is used. The resulting graph is shown in Figure 11.

From this result, it can be understood that the component in the test rig is still in the beginning of its fatigue life, with a very low fatigue usage after the component test with its 35k / 24.5k cycles. The mechanical test on the extracted specimens is performed at strain levels four times higher than in the component test, where the lifetime is at least a factor hundred shorter. This evaluation confirms that the effect of fatigue life reduction is not very significant in the studied component test.

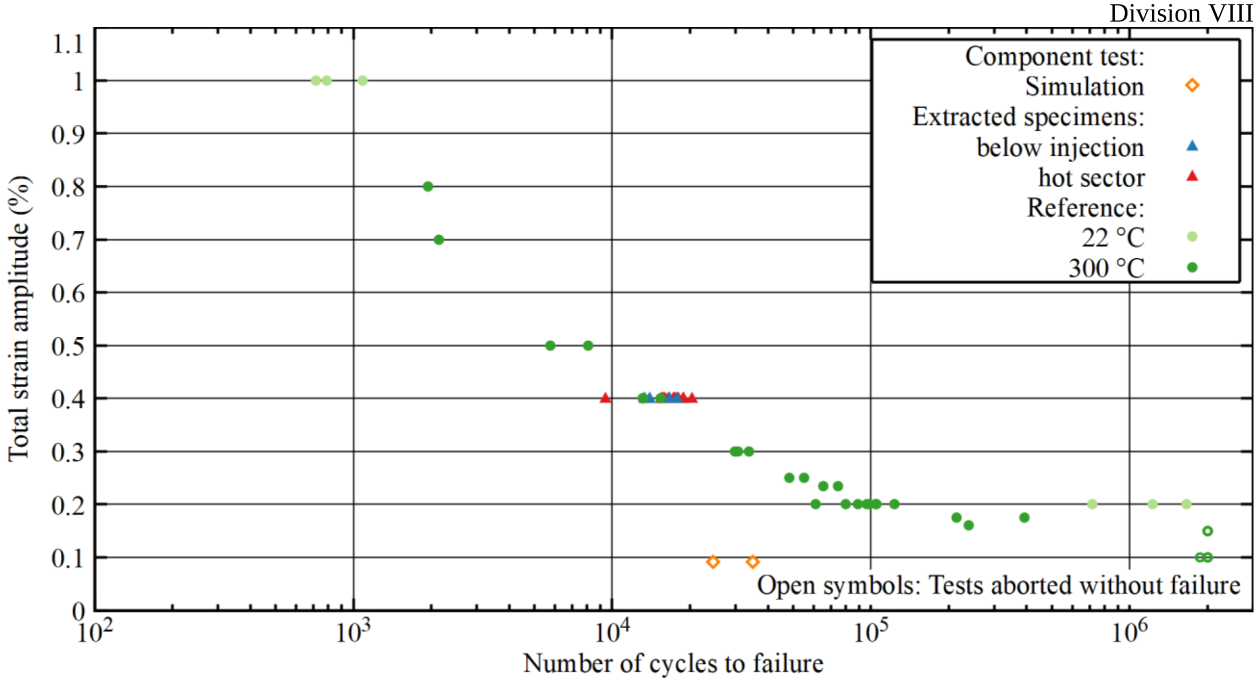

Figure 11. Fatigue life diagram for the component tests, the tests extracted specimens, and reference data (Rudolph et al., 2024, Smaga et al.,2024, Veile et al., 2024a, and Veile et al., 2024b).

SUMMARY AND CONCLUSION

The proposed test scheme allows for a controlled thermal degradation, which provides a component-level full-size test of thermal fatigue phenomena for piping components. The approach is demanding concerning the experimental setup and the quantification of thermal loads by simulations but allows for the validation of fatigue life curves gained by mechanical tests. Moreover, non-destructive techniques for the identification of fatigue degradation can be applied.

While the result is in accordance with the references and can be quantitatively understood, it has to be stated, that the component fatigue test reached only a level of relatively low fatigue degradation. This low fatigue usage after the test makes it challenging to characterize and quantify the degradation in the test. This result is also caused by the technical limitations of the full-size test: While the total number of cycles can only be increased by additional weeks of energy-intensive thermal testing, the load amplitude is limited by the hot water temperature, which is, due to the properties of water, restricted by the design pressure of the test rig (and also by the heating power).

ACKNOWLEDGEMENT

The work was carried out in the frame of a nuclear safety research project funded by the Federal Ministry for the Environment, Nature Conservation, Nuclear Safety and Consumer Protection (BMUV) within the framework of the joint project “Microstructure-based determination of the maximum service life for corrosion fatigue loaded materials and components of nuclear technology”, part II, project numbers 1501610A, 1501610B, 1501610C, 1501610D and RS1594E.

REFERENCES

Arndt, J., Heckmann, K., Sievers, J., Schopf, T., Silber, F.E., Veile, G., Weihe, S., Donnerbauer, K., Macias Barrientos, M., Walther, F., Bill, T., Starke, P., Acosta, R., Yerappa, B., Boller, C. (2024). "Thermo-mechanical FE simulations on a full-size thermal fatigue pipe test in view of lifetime assessment," *Transaction SMiRT-27*, Yokohama, Japan.

Ballesteros, A., Sanda, R., Peinador, M., Zerger, B., Negri, P., Wenke, R. (2014). "Analysis of events related to cracks and leaks in the reactor coolant pressure boundary," *Nuclear Engineering and Design*, 275, 163-167, doi:10.1016/j.nucengdes.2014.05.014.

Chopra, O., Stevens, G., (2018). "Effect of LWR Water Environments on the Fatigue life of Reactor Materials", Office of Nuclear Regulatory Research, NUREG/CR-6906, Rev. 1.

Donnerbauer, K., Koch, L.A., Veile, G., Silber, F., Weihe, S., Weber, F., Starke, P., Yerappa, B., Boller, C., Arndt, J., Heckmann, K., Sievers, J., Walther, F. (2024). "Fatigue damage evaluation of a metastable austenitic steel AISI 347 pipe after fluid structure interaction testing," *MPA-Seminar*, Stuttgart, Germany.

Heckmann, K., Acosta, R., Bill, T., Donnerbauer, K., Boller, C., Sievers, J., Macias Barrientos, M., Walther, F., Starke, P. (2023). "Detection of fatigue degradation in austenitic stainless steel with eddy current probe and machine learning," *Journal of Materials Research and Technology*, 27, 7336-7346, doi:10.1016/j.jmrt.2023.11.176.

Hong, J. N., Kim, J. W., Lee, D. Y., Lee, J.-M., Kim, Y.-J. (2023). „Very low-cycle fatigue failure behaviours of pipe elbows under displacement-controlled cyclic loading," *Thin-Walled Structures*, 193, 111261, doi:10.1016/j.tws.2023.111261.

Lydell, B., Escrig Forano, D., Riznic, J. (2021). "OECD nuclear energy agency CODAP database project on passive component operating experience. An international collaboration in materials research," *Nuclear Engineering and Design*, 380, 111280, doi:10.1016/j.nucengdes.2021.111280.

Nuclear Energy Agency (NEA), OECD (2019). "A Review of the 'Post-1998' Experience with Thermal Fatigue in Heavy Water and Light Water Reactor Piping Components," NEA/CSNI/R(2019)13, OECD/NEA.

Rudolph, J., Veile, G., Regitz, E:, Smaga, M., Fischer, U., Grimm, M., Weihe, S., Beck, T. (2024). „Investigation of the very high cycle fatigue (VHCF) behavior of AISI 347 and 304L austenitic stainless steels including their welds for reactor internals at ambient and operating temperature," *ASME PVP Conference*, PVP2024-121778, doi:10.1115/PVP2024-121778.

Smaga, M., Daniel, T., Regitz, E., Beck, T., Schopf, T., Veile, G., Weihe, S., Rudolph, J., Fisher, U. (2022). „Very high cycle fatigue (VHCF) behavior of austenitic stainless steels and their welds for reactor internals at ambient and operating relevant temperature,", *Transactions SMiRT-26*, Berlin/Potsdam, Germany.

Solin, J. (2024). "Environmental Fatigue – Early Results Revisited," ASME 2024 PVP Conference, Bellevue, Washington, USA, PVP2024-123450, doi:10.1115/PVP2024-123450

Solin, J., Seppänen, T. (2024). "EAF, Transferability to Operation and Improving Prospects," ASME 2024 PVP Conference, Bellevue, Washington, USA, /PVP2024-123437, doi:. 10.1115/PVP2024-123437.

Veile, G., Regitz, E., Smaga, M., Weihe, S., Beck, T. (2024a). „Investigations of metallurgical differences in AISI 347 and their influence on deformation and transformation behaviour and resulting fatigue life," *Materials*, 17 4543, doi:10.3390/ma17184543.

Veile, G., Regitz, E., Rudolph, J., Schopf, T., Smaga, M., Fischer, U., Grimm, M., Patzer, M., Weihe, S., Beck, T. (2024b). „Investigating very high cycle fatigue behavior of AISI 347 and 304L including their welds for reactor internals at ambient and operating relevant temperatures," *Transactions SMiRT-27*, Yokohama, Japan.

Weihe, S., Silber, S., Schopf, T, Swacek, C. (2022). „Investigations on the fatigue behavior of a full-scale pipe component with dissimilar weld under thermo-mechanical loading," *Transactions SMiRT-26*, Berlin/Potsdam, Germany.